Avrupa Bilim ve Teknoloji Dergisi
Sayı 17, S. 692-702, Aralık 2019

Araştırma Makalesi

www.ejosat.com ISSN:2148-2683

European Journal of Science and Technology
No. 17, pp. 692-702, December 2019

Research Article

The Effects of Initial *y plus*: Numerical Analysis of 3D NACA 4412 Wing Using *γ-Re$_\theta$ SST* Turbulence Model

Durmuş Sinan Körpe [1], Özdemir Öztürk Kanat [2*], Tuğrul Oktay [3]

[1] University of Turkish Aeronautical Association, Aeronautical Engineering, Ankara, Turkey (ORCID: 0000-0002-7968-4999)
[2] Kastamonu University, School of Civil Aviation, Department of Airframe and Powerplant Maintenance, Kastamonu, Turkey (ORCID: 0000-0001-7914-0871)
[3] Erciyes University, Faculty of Aeronautics and Astronautics, Aeronautical Engineering, Kayseri, Turkey (ORCID: 0000 0003 4860 2230)

(İlk Geliş Tarihi 8 Ekim 2019 ve Kabul Tarihi 7 Kasım 2019)

(**DOI:** 10.31590/ejosat.631135)

ATIF/REFERENCE: Körpe, D. S., Kanat, Ö. Ö. & Oktay, T. (2019). The Effects of Initial *y plus*: Numerical Analysis of 3D NACA 4412 Wing Using *γ-Re$_\theta$ SST* Turbulence Model. *Avrupa Bilim ve Teknoloji Dergisi*, (17), 692-702.

Abstract

In this numerical study, the effects of the initial *y plus*, which is a dimensionless wall distance, on the results of aerodynamic coefficients of designed a wing using NACA 4412 airfoil are investigated. For this purpose, the wing is designed and external flow analysis is carried out according to constant altitude. ANSYS Fluent, which is a Computational Fluid Dynamics (i.e. CFD) program and solves the problems according to the Finite Volume Method (i.e. FVM), is used for external flow analysis. Pressure-based method is used for numerical studies. Thus, the differences of coefficients on the wall, which are the results of the change in the *initial y plus*, are calculated ideally. Because of one of the best methods to solve the problems on transition zone, *γ-Re$_\theta$ SST* turbulence model is used for this study. Using this model for each analysis, first element heights (i.e. the distance to the nearest wall) are calculated according to 9 different *y plus* (i.e. 1, 5, 10, 30, 45, 60, 75, 90, 105). According to the first element heights, the inflation layers are created on the wing and the 3D control volumes are formed along the boundary region. To be more comprehensible, orthogonal quality-skewness values, expressing the quality of control volumes, are presented for each boundary. The changes in lift coefficients and drag coefficients on the same wing according to these 9 different *y plus* are presented numerically. In addition, obtained results are evaluated and as described in the literature, it is observed that to calculate the aerodynamic forces with the *γ-Re$_\theta$ SST* turbulence model is directly proportional to the *initial y plus*. As a consequence, this paper demonstrates that there are obvious differences detection of separation and determination of reattach region of flow occurring on the wing according to the *initial y plus.*

Keywords: *y plus*, *γ-Re$_\theta$ SST*, Computational Fluid Dynamics, ANSYS Fluent.

Başlangıç *y plus* Değerinin Etkileri: *γ-Re$_\theta$ SST* Türbülans Modeli Kullanılarak 3D NACA 4412 Kanadının Sayısal Analizi

Öz

Bu sayısal çalışmada, boyutsuz bir kavram olan *y plus* değerinin NACA 4412 kanat profili kullanılarak tasarlanmış olan bir kanadın aerodinamik katsayı sonuçları üzerine olan etkileri araştırılmıştır. Bu amaçla, bir kanat tasarlanmış ve dış akış analizi sabit irtifa değerine göre yürütülmüştür. Bu dış akış analizleri için, bir hesaplamalı akışkanlar dinamiği (HAD) programı olan ve sonlu hacim metoduna göre problemleri çözen ANSYS Fluent programı kullanılmıştır. Sayısal çalışma için basınç-tabanlı metottan yararlanılmıştır. Böylelikle başlangıç *y plus* değerindeki değişimlerin bir sonucu olarak meydana gelen duvar üzerindeki katsayı farklılıkları en iyi şekilde

[*] Sorumlu Yazar: Kastamonu University, School of Civil Aviation, Department of Airframe and Powerplant Maintenance, Kastamonu, Turkey, ORCID: 0000-0001-7914-0871, ozturkkanat@gmail.com

hesaplanabilmiştir. Laminer-türbülanslı akış geçişlerinin olduğu akış problemlerini çözen en iyi modellerden biri olması nedeniyle bu çalışmada *γ-Reθ SST* türbülans modeli kullanılmıştır. 9 farklı *y plus* (1, 5, 10, 30, 45, 60, 75, 90, 105) değeri için duvar üzerindeki ilk eleman yükseklikleri (duvar üzerindeki en yakın katman) hesaplanmıştır. Bu ilk eleman yüksekliğine göre kanat üzerinde inflation katmanları ile hesap bölgesi boyunca 3 boyutlu kontrol hacimleri oluşturulmuştur. Daha anlaşılabilir olması için, her bir hesap bölgesi için oluşturulan kontrol hacimlerinin kalitesini ifade eden ortogonal kalite ile eğrilik değerleri sunulmuştur. Aynı kanat üzerindeki bu 9 farklı *y plus* değerine göre taşıma ve sürükleme katsayılarındaki değişimler grafiksel olarak belirtilmiştir. Bunlarla birlikte, elde edilen sonuçlar değerlendirilmiş ve literatürde de belirtildiği gibi *γ-Reθ SST* modeli kullanılarak aerodinamik kuvvetlerin hesaplanabilmesinin, başlangıç *y plus* değeri ile doğrudan orantılı olduğu gözlemlenmiştir. Sonuç olarak, kanat üzerinde meydana gelen akış ayrılmalarının tespitinde ve akışın tekrar tutunmasının belirlenmesinde *başlangıç y plus* değerine bağlı olarak belirgin farklılıkların olduğu bu çalışma ile ortaya konulmuştur.

Anahtar Kelimeler: *y plus, γ-Reθ SST,* Hesaplamalı Akışkanlar Dinamiği, ANSYS Fluent.

1. Introduction

The CFD system is applied by solving the basic fluid dynamics equations using a limited number of solution elements and finally applying them to the whole flow volume. One of the most accurate approach to achieving realistic results is the comparative application of numerical and experimental methods. CFD is a branch of fluid mechanics, where problems with fluid behavior are fundamentally solved and analyzed on the computer by numerical methods and algorithms. Moreover, it is an excellent method for complex flow analysis; however, there is a need for knowledge and experience to create digital network structures, define true boundary conditions and interpret results. CFD solution is a very good way to make analysis which are costly to be analysed experimentally. While laminar flow solutions are less complicated with CFD, to solve turbulent flows different turbulence models should be applied. Many factors can affect the accuracy of the results obtained with CFD. Examples of these are the proper formation of geometry, the grids being sufficient and compatible with each other, and the use of appropriate flow methods (Kanat et al., 2017). Jansson et al. (Jansson et al.,2012) used CFD method to simulate NACA 0012 wing profile. They used FVM to calculate aerodynamic forces for a range of angles of attack. At least, they compared the results to validate with experimental data. They mentioned that the CFD simulation had captured dramatically the stall region.

γ-*Reθ SST* model for transition prediction uses a local correlation-based approach. There are also two transport equations in the model (Langtry & Menter, 2009). These are; one for intermittency and one for the transition onset criterion in terms of momentum-thickness Reynolds number. Langtry and Menter (Langtry et al., 2015) first expressed the full formulation of the model in 2009. This model has had a wide range of applications both academically and industrially in the following years.

Korpe and Kanat (Korpe and Kanat, 2019) analysed the flow around a wing that has NACA 4412 airfoil in their study. They calculated the lift and drag coefficients of this wing, which they designed, at different angle of attack. They used two different numerical analysis programs in order to obtain the results. These are solver based on nonlinear lifting-line theory implemented into XLFR5 and ANSYS-Fluent. They used *γ-Reθ SST* as the turbulence model in ANSYS-Fluent program. When they compared their results, they stated that there was conformity. A wing of the same size was created using the NACA 4412 profile in a similar manner by reference to this work. Thus, the accuracy of CFD results can be compared.

Steed (Steed, 2011) used a NASA Trapezoidal Wing model in his study. The researcher used SST based laminar to transition model and compared the results with both fully turbulent SST and wind tunnel results. He stated that *y plus* should be less than 1 in order to obtain accurate results with transition model. In summary, he stated that the *γ-Reθ SST* transition turbulence model was in good agreement with experimental data. Aftab et al. (Aftab et al., 2016) tried to capture the laminar separation bubble in their study using the NACA 4415 profile for a low Reynolds number flow. Reynolds number was set to 120,000. One equation Spallart Allmars, two equation *kw SST*, three equation intermittency *(γ) SST, k-kl-w* and the four equation transition *γ-Reθ SST* in total 5 different turbulence model hev been tested. When comparing the results obtained using these models with each other and the experimental study, they stated that the best fit was achieved with the *γ-Reθ SST* model. They also emphasized that the correct turbulence model should be used in order to capture the transition behavior with the CFD study. In addition, they found that the *γ-Reθ SST* turbulence model can accurately and rapidly predict flow behavior for both low angle of attack and high angle of attack.

In this research article, CFD approach is implemented in order to investigate the effect of *initial y plus* over the aerodynamic forces (i.e. C_L and C_D). Furthermore, the effect of the turbulence model on the lift and drag coefficients according to the initial value of the first element height on the wall is focused.

2. Material and Method

2.1. *γ-Reθ SST Turbulence Model and y Plus*

Due to the low Reynolds number, γ-*Reθ SST* turbulence model was used to accurately estimate the flow. This model is also sometimes known as the Langtry-Menter 4-equation transitional *SST* model or *gamma-Retheta-SST* model. The difference of this model from the *kw-SST* turbulence model is that the *gamma* and *Retheta* equations have also been added. The transport equation for the intermittency (i.e. γ) is given as in Eqn. 1 (Menter et al., 2006).

$$\frac{\partial(\rho\gamma)}{\partial t}+\frac{\partial(\rho U_j\gamma)}{\partial x_j}=P_{\gamma1}-E_{\gamma1}+P_{\gamma2}-E_{\gamma2}+\frac{\partial}{\partial x_j}\left[\left(\mu+\frac{\mu_t}{\sigma_\gamma}\right)\frac{\partial\gamma}{\partial x_j}\right] \quad (1)$$

For the transition momentum thickness Reynolds number (i.e. $R\tilde{e}_{\theta t}$) , the transport equation is defined as follows:

$$\frac{\partial(\rho R\tilde{e}_{\theta t})}{\partial t}+\frac{\partial(\rho U_j R\tilde{e}_{\theta t})}{\partial x_j}=P_{\theta t}+\frac{\partial}{\partial x_j}\left[\sigma_{\theta t}(\mu+\mu_t)\frac{\partial R\tilde{e}_{\theta t}}{\partial x_j}\right] \quad (2)$$

Coupling of the transition model with *shear stress transport (i.e. SST) kw* by modification of *k*-equation is given as follows:

$$\frac{\partial}{\partial t}(\rho k)+\frac{\partial}{\partial x_i}(\rho k u_i)=\frac{\partial}{\partial x_j}\left[\Gamma_k\frac{\partial k}{\partial x_j}\right]+G_k^*-Y_k^*+S_k \quad (3)$$

$$G_k^*=\gamma_{eff}\tilde{G}_k \quad (4)$$

$$Y_k^*=min\left(max\left(\gamma_{eff},0.1\right),1.0\right)Y_k \quad (5)$$

Y plus value is dimensionless and the formula is as follows (Nichols, 2010):

$$y\,plus=\frac{\vartheta^* y}{V} \quad (6\ )$$

In Eqn. 6, the *y* term is the distance of the viscous region on the wing or wall where the flow will be. ϑ^* is the friction velocity, V is the kinematic viscosity. A desired *y plus* value is determined before starting the calculation and according to this, the first element height is calculated by using kinematic viscosity with friction velocity (Bredberg, 2000). The first element heights of the inflation layers were calculated based on this formula. In table 1, the characteristics of elements created by calculating the different first element heights according to the *y plus* value is given.

Table 1. The Cell Properties

Initial *y plus*	First Layer Height	Inflation Layers	Maximum Skewness	Minimum Orthogonal Quality	Elements
1(Korpe and Kanat, 2019)	1.5×10^{-5}	61	0.95	2.9×10^{-3}	2 569 785
5	7.6×10^{-5}	40	0.93	1.3×10^{-2}	2 013 222
10	1.5×10^{-4}	36	0.91	2.4×10^{-2}	1 868 237
30	4.4×10^{-4}	28	0.92	9.2×10^{-2}	1 605 355
45	6.7×10^{-4}	22	0.93	0.12	1 457 725
60	9.1×10^{-4}	20	0.95	0.12	1 391 046
75	1.1×10^{-3}	15	0.91	0.14	1 288 856
90	1.4×10^{-3}	13	0.91	0.14	1 231 853
105	1.6×10^{-3}	11	0.94	0.15	1 188 780

2.2. *Geometry, Grid and Setup*

For geometry, a 3-D solid model was first created using the NACA 4412 profile. In order to ensure independence from boundary around this model, a solution domain of approximately 30 times has been created (Thomas & Salas, 1986). Figure 1 shows the solution domain with the formed wing. While creating the solution domain, it has been paid attention that it is the optimum size. It is aimed to ensure independence from the designed domain and to ensure that the solution time is at minimum with optimum value.

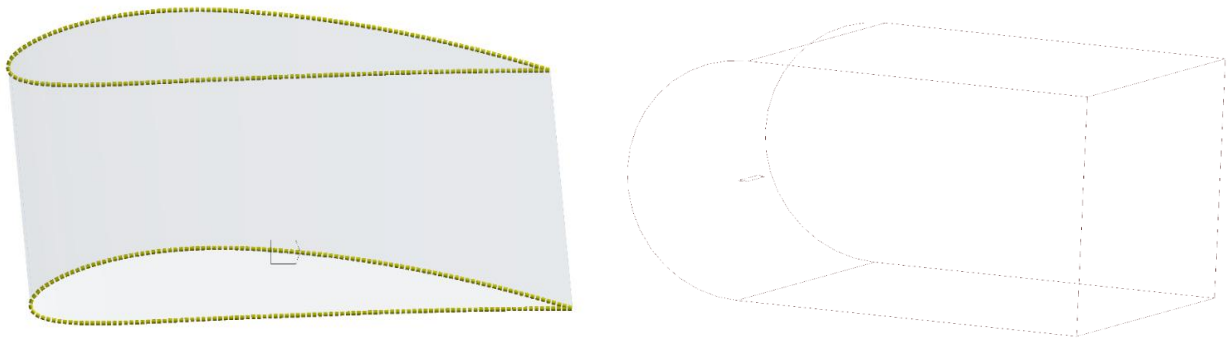

(a) *(b)*

Figure 1. (a). Airfoil (b). Solution Domain

Another step that needs to be taken into consideration in order to get the correct results in the solution is control volumes. Due to the numerical analysis of the 3-dimensional shape, 3-dimensional cells have been created. Prism and inflation layers are used and therefore created cells are hybrid. For the accuracy of the results, volumetric compatibility is considered for the transition region after the last inflation layers.

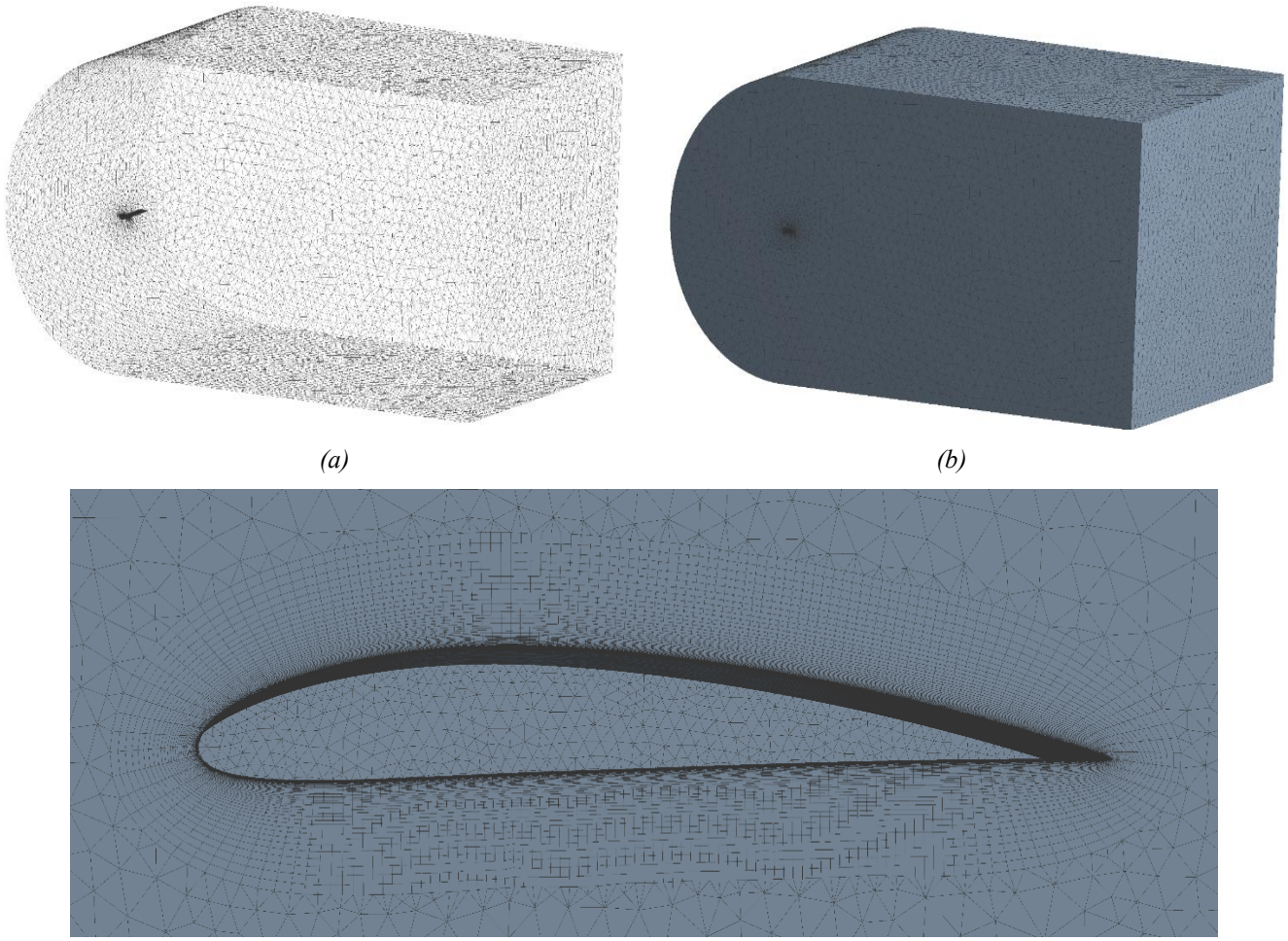

(a) *(b)*

(c)

Figure 2. (a).Wireframe View (b).Control Volumes (c).Cells Around The Airfoil (y plus=1)

Another important criterion that is decisive in the solution is the turbulence model used for performing numerical analysis. In order to make a model decision, it is necessary to know whether the flow is turbulent or laminar flow. Whether the flow is laminar flow or turbulent can be determined by looking at the Reynolds number (Sinorri, 2014). The Reynolds number is defined as the ratio of the inertial forces of a fluid to the viscosity forces. For this reason, the Reynolds number of the flow was calculated as in Eqn. 9 by using Eqn. 7. Based on the result and taking into account Eqn. 8, it is a combination of laminar and turbulent flow (Bertin & Russell, 2014). In this study, air velocity is accepted as 22 m / s.

$$Re = \frac{\vartheta L \rho}{\mu} \tag{7}$$

$$3 \times 10^5 < Re < 3.5 \times 10^6 \tag{8}$$

$$Re = \frac{22 \times 0.45 \times 1.176}{1.7894 \times 10^{-5}} = 6.5 \times 10^5 \tag{9}$$

Each numerical analysis is calculated for 16 different angles of attack, -8, -6, -4, -2, 0, 2, 4, 6, 8, 10, 12, 14, 16, 18, 20, 22. At 1600 iterations the calculation is completed. This corresponds to a continuity value of 10^{-4} for 0 ° angle of attack.

3. Results and Discussion

Figure 3 shows the lift coefficient (C_L) results obtained from numerical analyzes performed using 9 different *y plus* values according to 16 different angle of attack. When these results are compared, it is seen that the changes in the *initial y plus* cause significant deviations over the results as the angle of attack increases. In addition, the changes in the stall angle of the wing (i.e. C_{Lmax}) accordingly to this are support this situation. When *y plus* 1 (Korpe and Kanat, 2019) results is evaluated, it is seen that the decrease in the lift coefficient of the wing starts at 20° angle of attack. According to the results, as *y plus* increases, the stall angle of the wing decreases to 14 degrees.

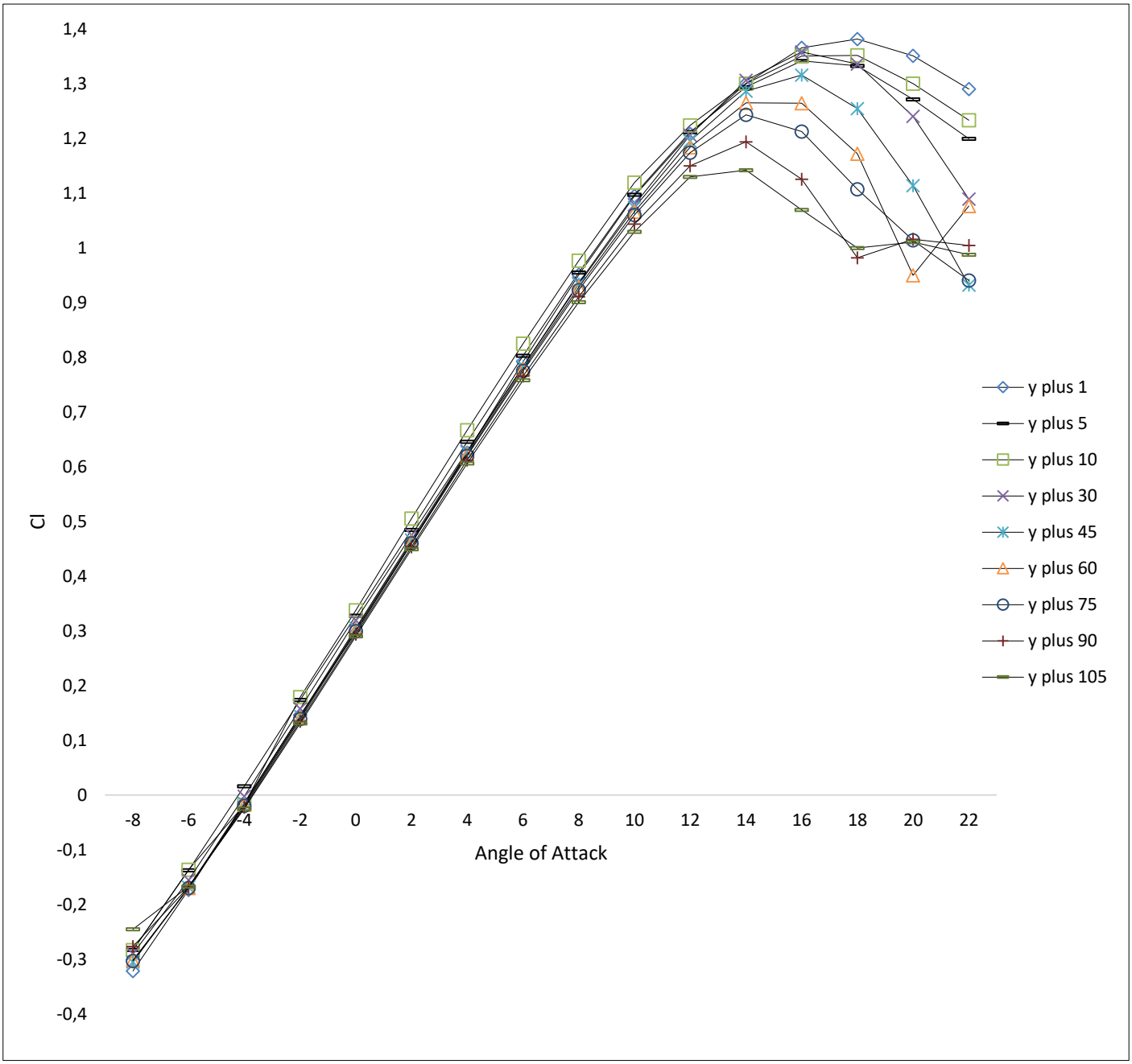

Figure 3. C_L Coefficients

When Figure 4 is evaluated, it is seen that there is a parallelism in the results obtained between -6 ° angle of attack and 12 ° angle of attack. This parallelism changes at angles greater than 12 ° angle of attack and the calculated C_D coefficients show more differences. Similarly, the differences in the calculated C_D coefficients increase at the-8° angle of attack. In short, the difference between the C_D coefficients calculated in a given range of angle of attack remains constant even if the *initial y plus* values are different.

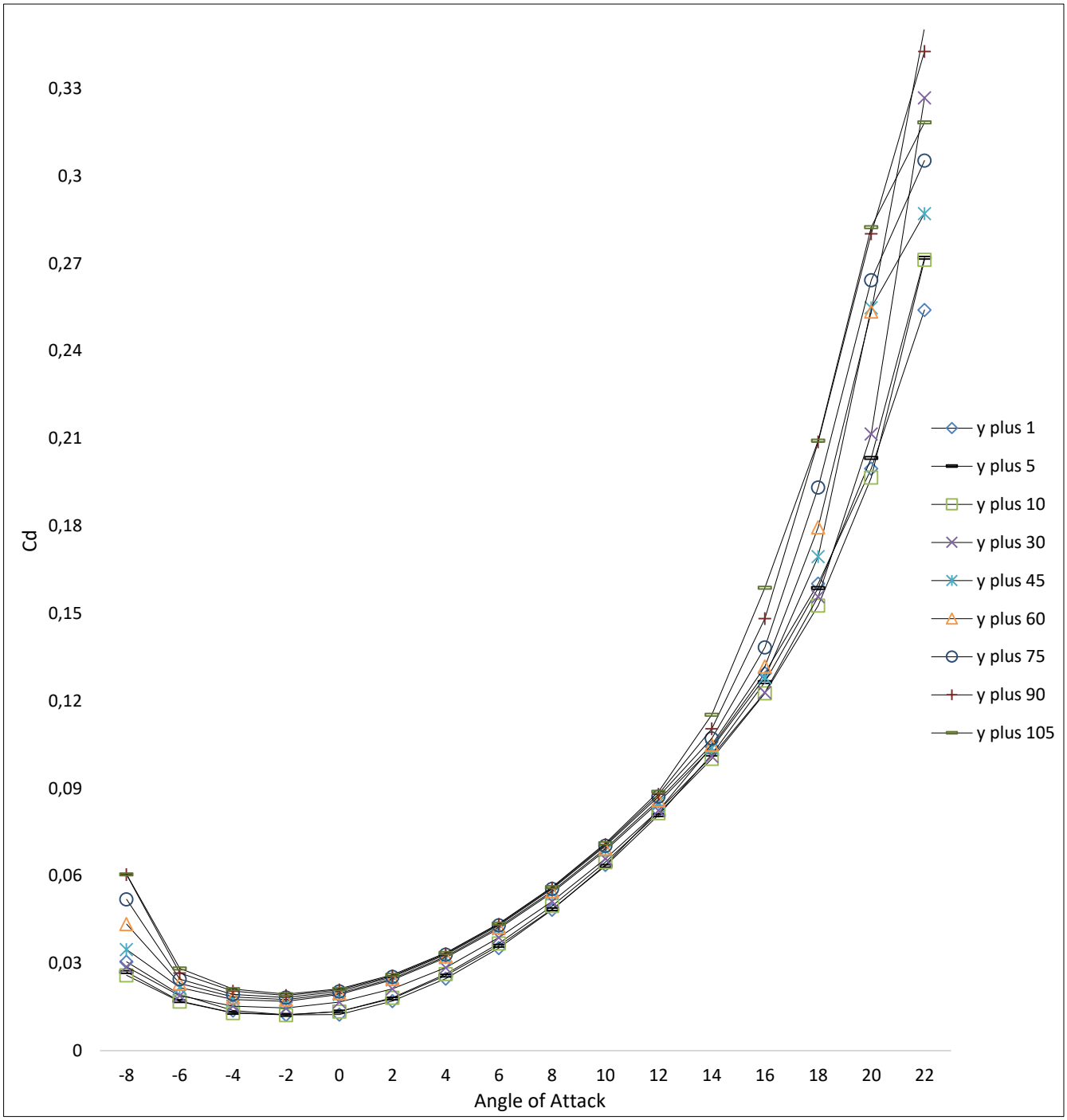

Figure 4. C_D Coefficients

Figure 5 shows the *final y plus* contours obtained according to the *initial y plus*. As seen in th figüre, all of the *final y plus* results were calculated using γ-Re_θ SST turbulence model as smaller than initial values. As the *y plus* value increases, the convergence on the wing decreases.

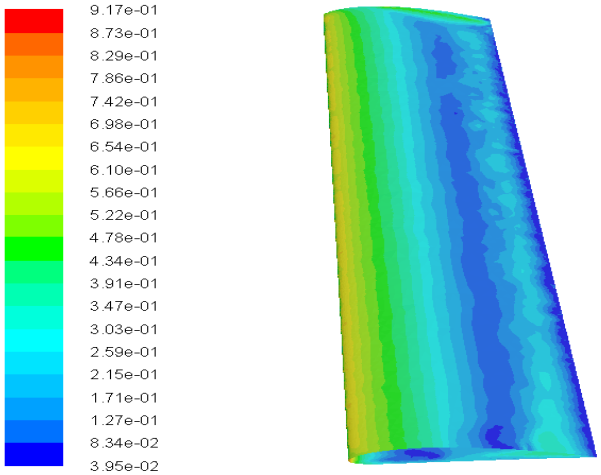
9.17e-01
8.73e-01
8.29e-01
7.86e-01
7.42e-01
6.98e-01
6.54e-01
6.10e-01
5.66e-01
5.22e-01
4.78e-01
4.34e-01
3.91e-01
3.47e-01
3.03e-01
2.59e-01
2.15e-01
1.71e-01
1.27e-01
8.34e-02
3.95e-02

(a)

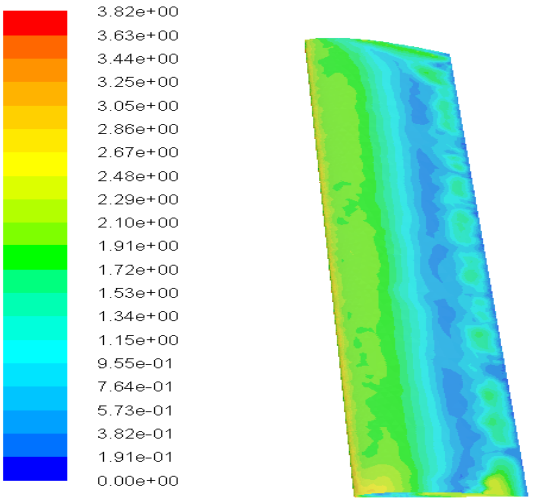
3.82e+00
3.63e+00
3.44e+00
3.25e+00
3.05e+00
2.86e+00
2.67e+00
2.48e+00
2.29e+00
2.10e+00
1.91e+00
1.72e+00
1.53e+00
1.34e+00
1.15e+00
9.55e-01
7.64e-01
5.73e-01
3.82e-01
1.91e-01
0.00e+00

(b)

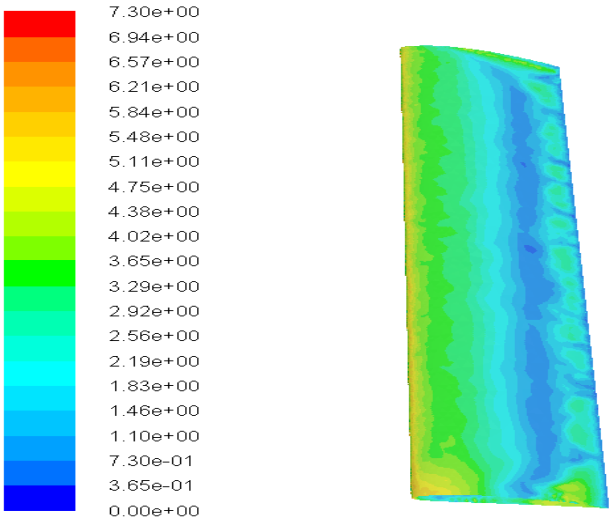
7.30e+00
6.94e+00
6.57e+00
6.21e+00
5.84e+00
5.48e+00
5.11e+00
4.75e+00
4.38e+00
4.02e+00
3.65e+00
3.29e+00
2.92e+00
2.56e+00
2.19e+00
1.83e+00
1.46e+00
1.10e+00
7.30e-01
3.65e-01
0.00e+00

(c)

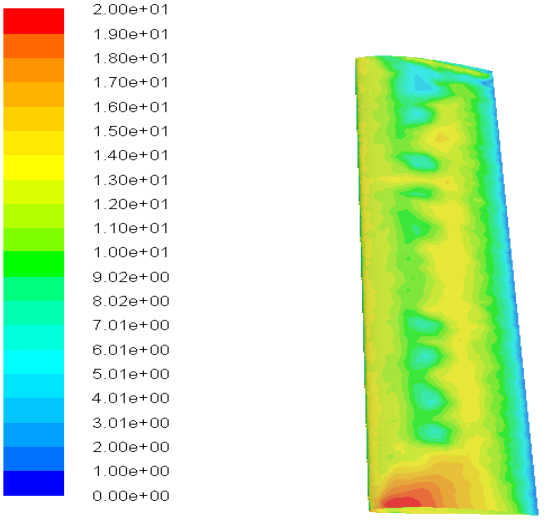
2.00e+01
1.90e+01
1.80e+01
1.70e+01
1.60e+01
1.50e+01
1.40e+01
1.30e+01
1.20e+01
1.10e+01
1.00e+01
9.02e+00
8.02e+00
7.01e+00
6.01e+00
5.01e+00
4.01e+00
3.01e+00
2.00e+00
1.00e+00
0.00e+00

(d)

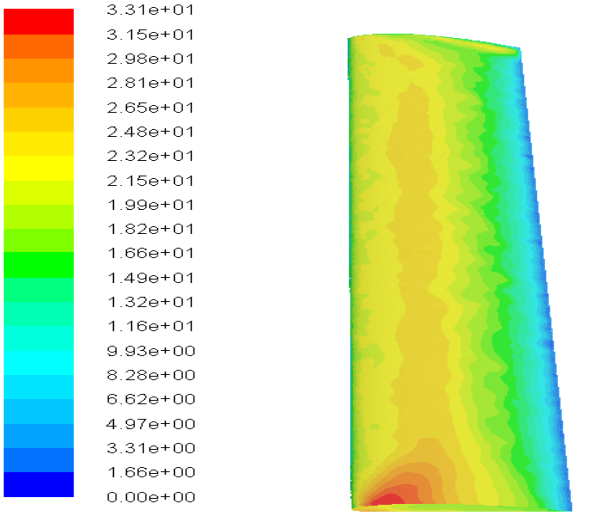
3.31e+01
3.15e+01
2.98e+01
2.81e+01
2.65e+01
2.48e+01
2.32e+01
2.15e+01
1.99e+01
1.82e+01
1.66e+01
1.49e+01
1.32e+01
1.16e+01
9.93e+00
8.28e+00
6.62e+00
4.97e+00
3.31e+00
1.66e+00
0.00e+00

(e)

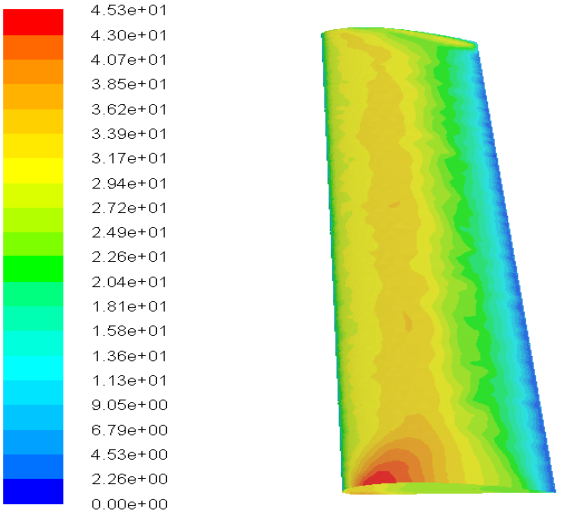
4.53e+01
4.30e+01
4.07e+01
3.85e+01
3.62e+01
3.39e+01
3.17e+01
2.94e+01
2.72e+01
2.49e+01
2.26e+01
2.04e+01
1.81e+01
1.58e+01
1.36e+01
1.13e+01
9.05e+00
6.79e+00
4.53e+00
2.26e+00
0.00e+00

(f)

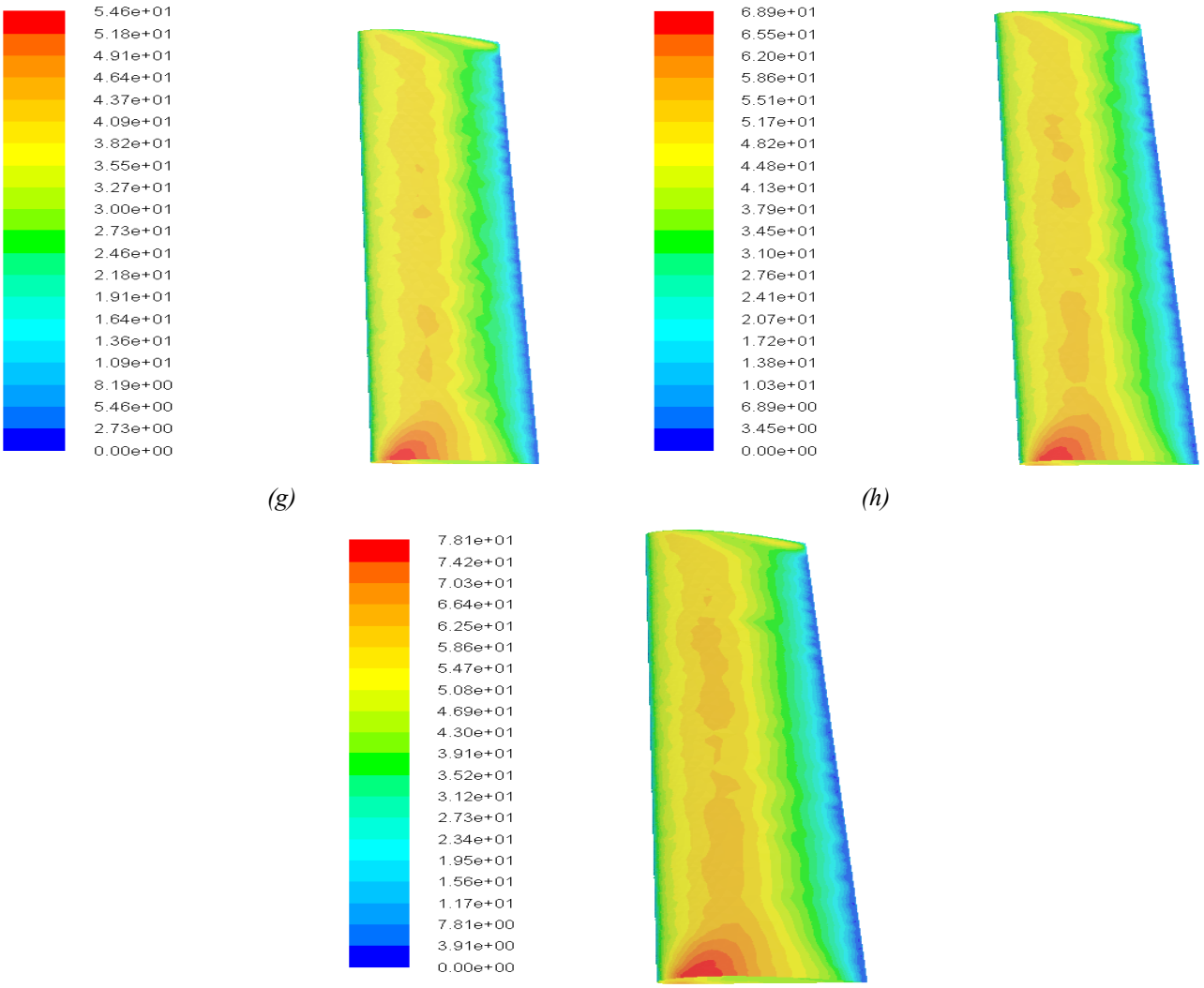

Figure 5. y plus Contours Respectively (a).1, (b).5, (c).10, (d).30, (e).45, (f).60, (g).75, (h).90, (ı).105

Figure 6 depicts the X Wall Shear Stress views obtained for all *initial y plus values* at 16° angle of attack. The view is 2-dimensional. It is formed as a profile from the midpoint of the designed wing. When the two views are compared, the separation points on the wing are clearly visible. The results show that for numerical analysis to be more accurate convergence is possible with a smaller initial y plus (for smaller first element height). Accordingly, a slight separation is observed at about half of the wing chord length for *initial y plus=1* after that it reattaches. A separation is observed again near the trailing edge. For bigger *initial y plus*, the separation on the wing begins earlier and nearly continues without reattach. This directly affects C_L and C_D results. Especially, the figüre depicts no reattach region on the airfoil for *initial y plus 90 and 105.*

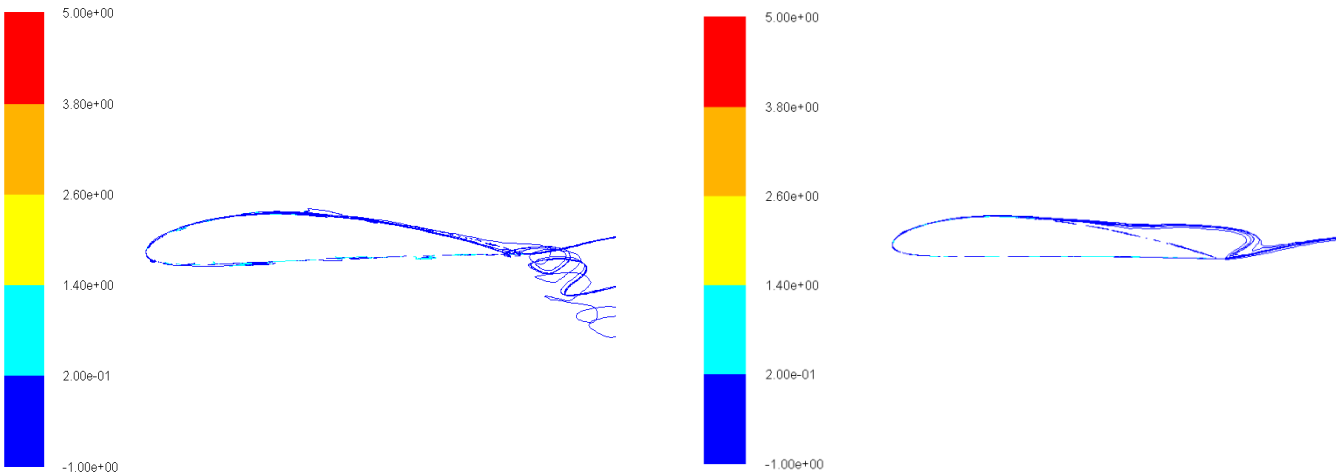

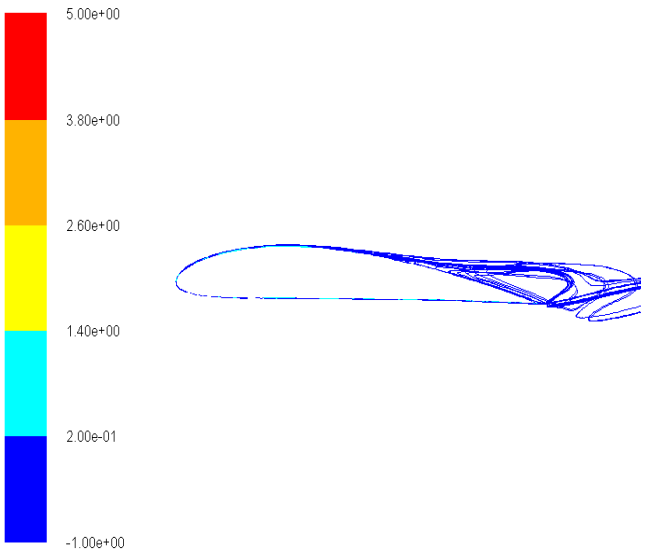
5.00e+00
3.80e+00
2.60e+00
1.40e+00
2.00e-01
-1.00e+00

(c)

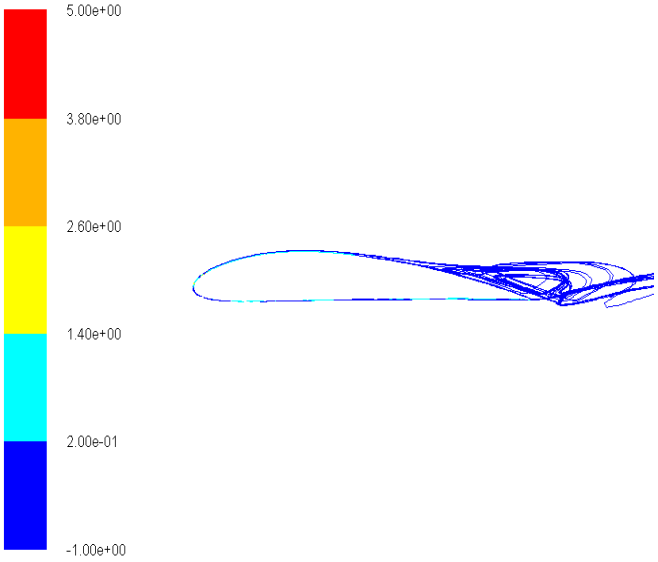
5.00e+00
3.80e+00
2.60e+00
1.40e+00
2.00e-01
-1.00e+00

(d)

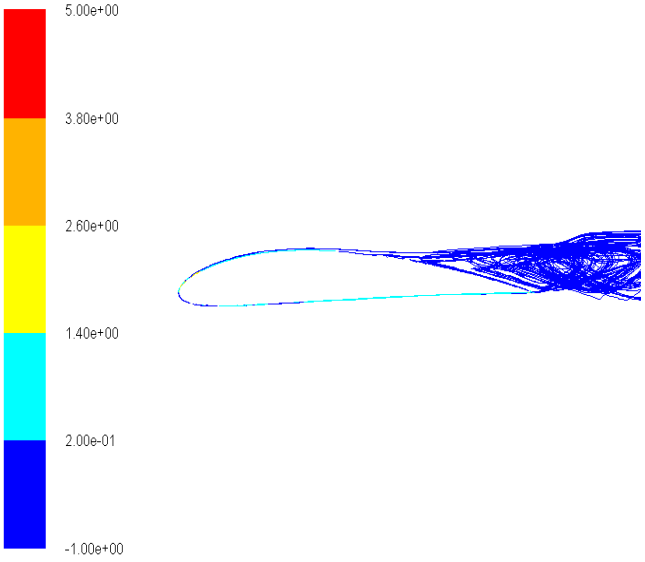
5.00e+00
3.80e+00
2.60e+00
1.40e+00
2.00e-01
-1.00e+00

(e)

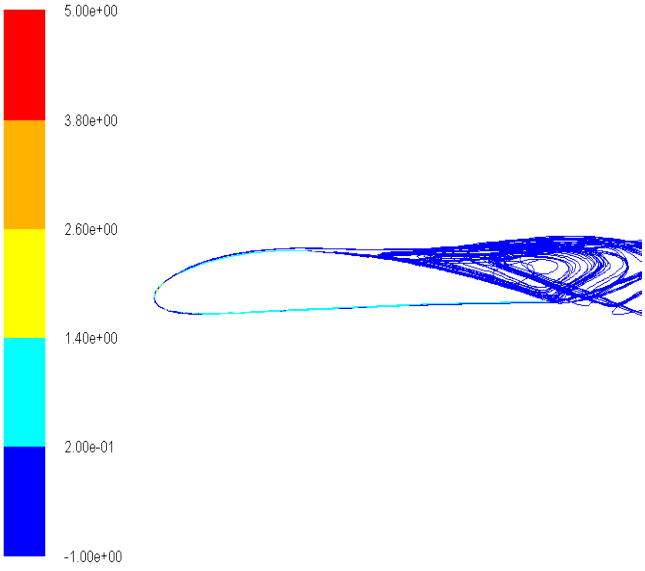
5.00e+00
3.80e+00
2.60e+00
1.40e+00
2.00e-01
-1.00e+00

(f)

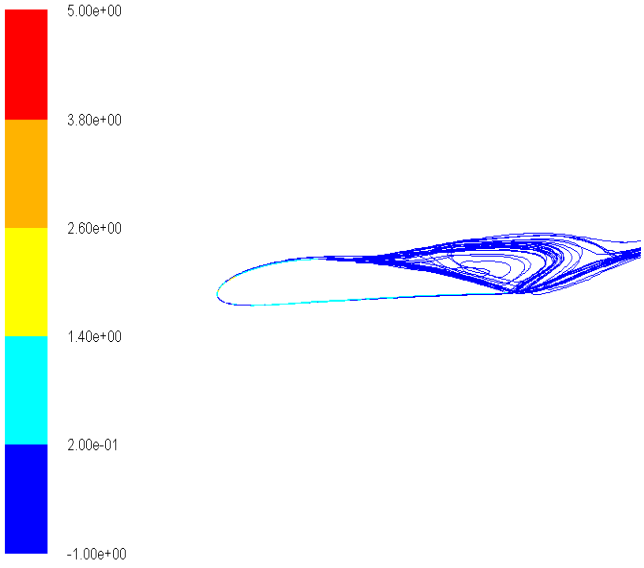
5.00e+00
3.80e+00
2.60e+00
1.40e+00
2.00e-01
-1.00e+00

(g)

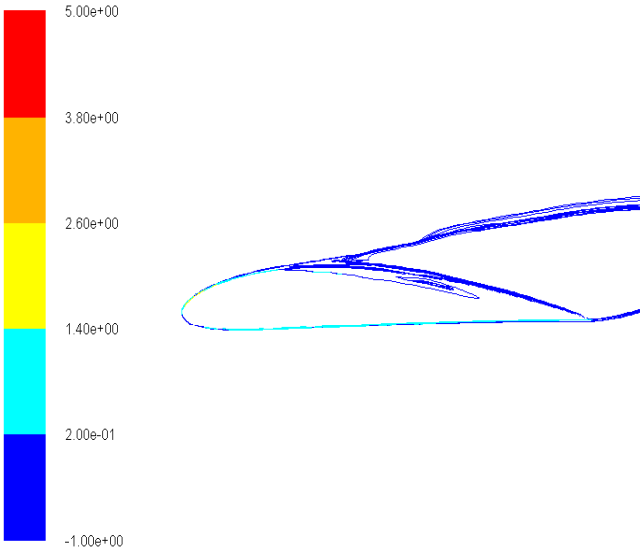
5.00e+00
3.80e+00
2.60e+00
1.40e+00
2.00e-01
-1.00e+00

(h)

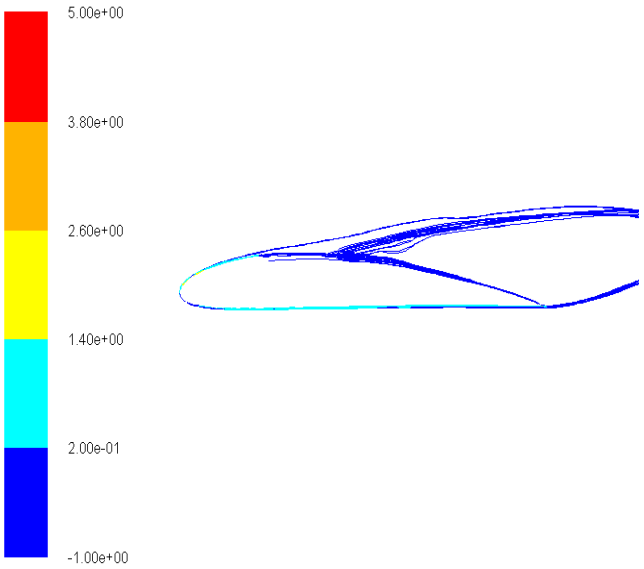

(ı)

Figure 6. X Wall Shear Stress Pathlines (Pascal) At 16° Angle of Attack For y plus, Respectively (a).1, (b).5, (c).10, (d).30, (e).45, (f).60, (g).75, (h).90, (ı).105

4. Conclusion

The effect of the *initial y plus* value is investigated for the C_L and C_D coefficients of a wing designed by using NACA 4412 airfoil with this study. The main contrubition of this research article to the literature is to have evaluated correlation between aerodynamic forces and *initial y plus*. Differences in C_L and C_D coefficients calculated for different *initial y plus* using the same wing are expressed both visually and graphically. In addition to this the flow throught the wing demonstrates differences. As the *initial y plus* decreases, the calculated separation region on the wing reach through the trailing edge of the wing. In particular, this paper demonstrates that there are obvious differences in both detection of separation and determination of reattach region of flow occurring on the wing at high angle of attack. As a results, these differences directly have effects of the calculation of aerodyanmic forces.

References

Aftab, S. M. A., Rafie, A. M., Razak, N. A. & Ahmad, K. A. (2016). Turbulence Model Selection For Low Reynolds Number Flows. *PloS one*, *11*(4), e0153755.

ANSYS Fluent Theory Guide, (2013).

Bertin, J. J. & Russell, M. C. (2014). Aerodynamics for Engineers Sixth Edition, Pearson Education Limited, London.

Bredberg, J. (2000). On the Wall Boundary Condition for Turbulence Models. Department of Thermo and Fluid Dynamics, Chalmers University of Technology, Göteborg, Sweden (p. 21).

Jansson, J., Hoffman, J., & Jansson, N. (2012). Simulation of 3d unsteady incompressible flow past a naca 0012 wing section.

Kanat, O. O., Korpe, D. S. & Kurban, A. O. (2017). Yatay Kuyruklarda Kıvrık Kanat Ucu Kullanımının Aerodinamik Etkileri. *Journal of Aviation*, *1*(2), 87-98.

Körpe, D. S. & Kanat, Ö. Ö. (2019). Aerodynamic Optimization of a UAV Wing subject to Weight, Geometric, Root Bending Moment, and Performance Constraints. *International Journal of Aerospace Engineering*, 2019.

Langtry, R. (2015). Extending the Gamma-Rethetat Correlation Based Transition Model for Crossflow Effects. *In 45th AIAA fluid dynamics conference* (p. 2474).

Langtry, R. B. & Menter, F. R. (2009). Correlation-based transition modeling for unstructured parallelized computational fluid dynamics codes. *AIAA journal*, *47*(12), 2894-2906.

Menter, F. R., Langtry, R. B., Likki, S. R., Suzen, Y. B., Huang, P. G. & Völker, S. (2006). A Correlation-Based Transition Model Using Local Variables—Part I: Model Formulation. *Journal of Turbomachinery*, 128(3), (p. 413).

Nichols, R. H. (2010). Turbulence models and their application to complex flows. *University of Alabama at Birmingham, Revision*, *4*, 89.

Snorri, G. (2014). General Aviation Aircraft Design: Applied Methods and Procedures. Butterworth-Heinemann is an imprint of Elsevier, USA.

Steed, R. (2011). High Lift CFD Simulations With An SST-Based Predictive Laminar to Turbulent Transition Model. In *49th AIAA Aerospace Sciences Meeting including the New Horizons Forum and Aerospace Exposition* (p. 864).

Thomas, J.L. & Salas, M.D. (1986). Far-Field Boundary Conditions For Transonic Lifting Solutions to the Euler Equations. *AIAA Journal,* Vol. 24, No. 7, (p. 1074).